

We are IntechOpen, the world's leading publisher of Open Access books Built by scientists, for scientists

6,900

Open access books available

185,000

International authors and editors

200M

Downloads

Our authors are among the

154

Countries delivered to

TOP 1%

most cited scientists

12.2%

Contributors from top 500 universities



WEB OF SCIENCE™

Selection of our books indexed in the Book Citation Index
in Web of Science™ Core Collection (BKCI)

Interested in publishing with us?
Contact book.department@intechopen.com

Numbers displayed above are based on latest data collected.
For more information visit www.intechopen.com



Recent Developments in the Study of the Behavior of Fluorescent Membrane Probes in Lipid Bilayers: Molecular Dynamics Approach

Luís M.S. Loura^{1,2}, A.J. Palace Carvalho^{3,4} and J.P. Prates Ramalho^{3,4*}

¹*Centro de Química de Coimbra, Universidade de Coimbra, Coimbra,*

²*Faculdade de Farmácia, Universidade de Coimbra,*

Pólo das Ciências da Saúde, Azinhaga de Santa Comba, Coimbra,

³*Centro de Química de Évora, Universidade de Évora, Évora,*

⁴*Departamento de Química, Universidade de Évora, Évora, Portugal*

1. Introduction

The molecular level organization of biomembranes and the establishment of structure/function relationships of membrane-active biomolecules are topics of crucial importance for the understanding of many phenomena in cell biophysics and biochemistry. This poses challenging problems that most frequently require the use of advanced experimental techniques (Gennis, 1989), among which fluorescence stands out as one of the most powerful and commonly used due to its sensitivity and versatility (Lakowicz, 2006; Royer & Scarlata, 2008). The sub-nanosecond time resolution of fluorescence allows following the kinetics of both fast (fluorophore rotation, conformational changes) and relatively slow (translocation, hindered diffusion) processes, and its extremely high sensitivity (as evidenced in techniques such as single-fluorophore imaging and fluorescence correlation spectroscopy) is almost unrivaled. But, perhaps the most salient feature of fluorescence spectroscopy is its high versatility which allows, through different parameters, the retrieval of complementary molecular information on the system under study. Spectral and fluorescence lifetime/quantum yield variations are informative regarding the polarity and/or solvent accessibility of the fluorophore microenvironment and the extent of partition of a fluorophore-bearing molecule between the aqueous and membrane media, or between coexisting membrane phases or domains. Fluorescence quenching, depending on the underlying interaction mechanism and on the experimental design, can be used to study molecular aggregation, lateral diffusion, compartmentalization, or transverse location in the bilayer. Fluorescence polarization is used to measure the viscosity of the microenvironment and the kinetics of fluorophore rotation. Förster resonance energy transfer (FRET) is useful in many common situations, such as detection and characterization of membrane heterogeneity, determination of the transverse location of protein fluorophores, detection

* Corresponding Author

and quantification of protein/lipid selectivity, and characterization of protein oligomerization. Fluorescence microscopy adds spatial resolution to the canon, and, also because of the non-destructive nature of fluorescence techniques, is widely used in the study of live cells (Royer & Scarlata, 2008; de Almeida et al. 2009). An increasing number of laboratories all over the world are equipped with instruments capable of measuring microscopic fluorescence decays, thus combining spatial and time resolution. In particular, recent developments in multi-wavelength and polarization resolved imaging have led to a widespread use of FRET imaging in studies of functional assemblies in cell membranes (de Almeida et al., 2009).

The basic structural unit of biological membranes is the phospholipid bilayer, and because the vast majority of naturally occurring membrane lipids are non-fluorescent, many of the applications described above require the use of extrinsic membrane probes containing fluorophores with convenient photophysical properties, such as absorption and emission in the visible range and high molar absorption coefficient and fluorescence quantum yield (which is especially convenient for microscopy and single-molecule techniques). Some fluorophores are known for their simple decay kinetics, stability, and invariance of fluorescence parameters, while others are notable for their sensitivity to the local environment. Taking into account the purpose of a given experiment, either one of these types of molecules will be most appropriate (Maier et al., 2002). Some of these fluorescence membrane probes bear no resemblance to lipids, but due to their hydrocarbon-based structure, are sufficiently hydrophobic to partition to the lipid environment. Examples described below are 1,6-diphenyl-hexatriene (DPH) or pyrene (see Fig. 1A and Fig. 1B for structures). Sometimes, synthetic fluorophores are attached to aliphatic chains to increase the extent of partition. In other cases, the probes are phospholipids with a suitable fluorophore covalently attached to either the polar headgroup or one of the acyl chains, or sterols with a fluorophore label bound to either the side chain or the oxygen atom (e.g. cholesteryl esters). In all cases, the probe is a foreign molecule inserted in a host lipid matrix.

Two major issues arise regarding the use of extrinsic probes in membrane studies. First, the behavior of the probe molecule inside the bilayer (e.g. what transverse region of the bilayer is the probe sensitive to, its translational and rotational dynamics) is often not fully understood. Second, when interpreting the results of fluorescence experiments, it can be hard to distinguish between legitimate membrane properties and the perturbing effects resulting from incorporation of the probe (in bilayer structure, dynamics of bilayer components and thermotropic behavior) even in low concentrations (Bouvrais et al., 2010). Whereas the first point can be addressed experimentally using suitable fluorescence techniques (e.g., differential quenching, dynamical self-quenching, time-resolved anisotropy), the latter issue is best dealt with using a methodology able to simultaneously monitor the probe and lipid molecules independently. Given the sheer amount of work that has been carried out using fluorescent membrane probes, it is surprising to note the scarcity of studies that have addressed this fundamental matter.

Molecular dynamics (MD) simulations can provide detailed atomic-scale information, and have been extensively used in the study of lipid bilayer structure and dynamics (Ash et al., 2004; Berkowitz, 2009). This technique has also been established in the past decade as a method of choice to analyze both the location and dynamics of membrane probes and the extent of perturbation they induce in the host bilayer. Fluorophore properties that can be

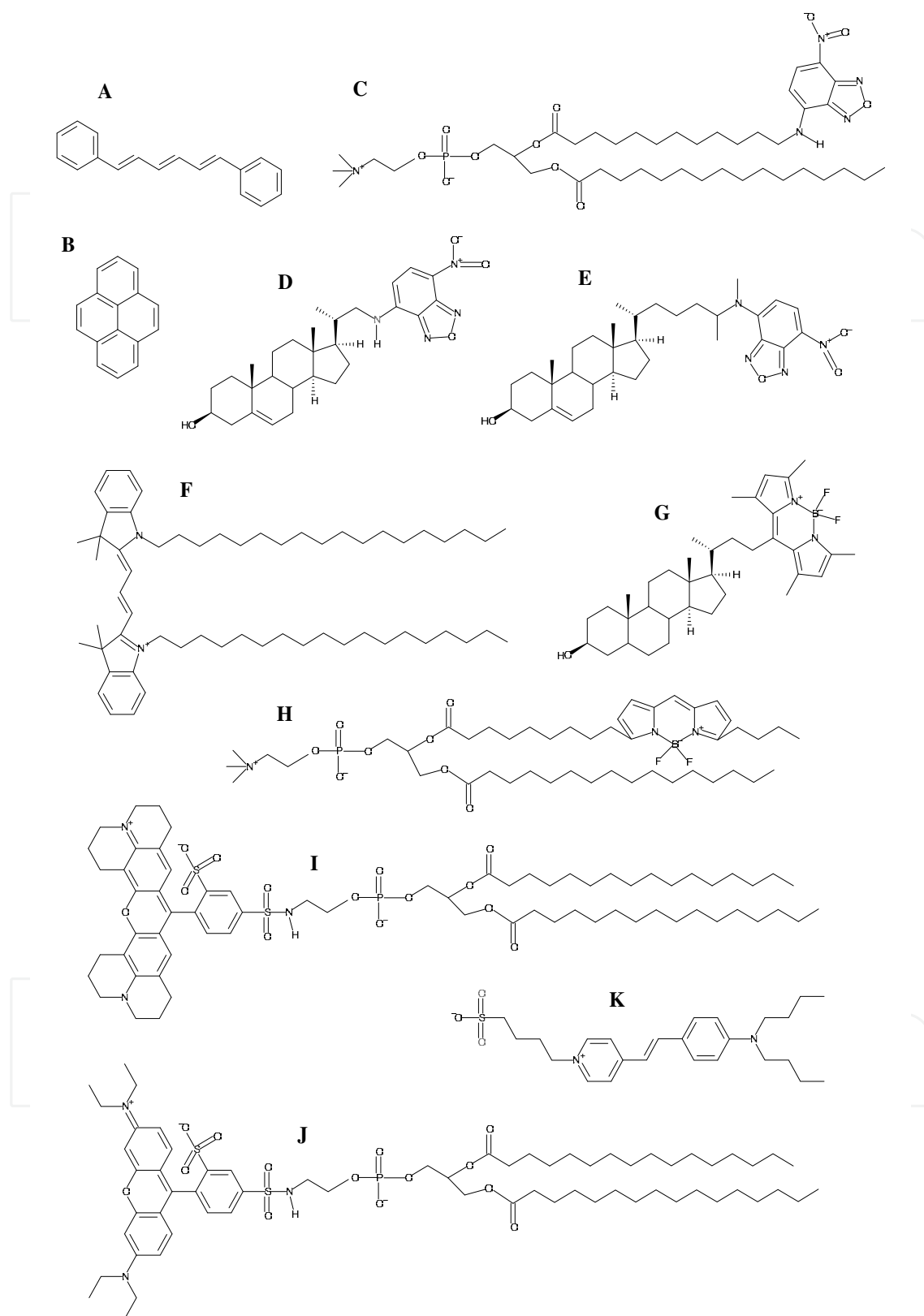


Fig. 1. Structures of membrane probes mentioned in this chapter. (a) DPH; (b) pyrene; (c) C12-NBD-PC; (d) 22-NBD-cholesterol; (e) 25-NBD-cholesterol; (f) DiI; (g) BODIPY-cholesterol; (h) BODIPY-PC; (i) TR-DHPE; (j) Rhod-DPPE; (k) Di-4-ASPBS.

monitored in MD simulations include mass distribution, conformation/orientation, extent of solvation/hydrogen bonding, radial distribution functions, rotational/translational dynamics, and aggregation state. On the other hand, bilayer parameters include area per lipid, density profiles, translational and rotational (headgroup, acyl chain) dynamics, order parameters, orientation of water molecules and lipid headgroups at the interface, and electrostatic potential across the membrane. Comparison between simulations in presence and absence of bilayer-incorporated probe allows evaluation of the perturbation induced by the latter. For the purpose of validating the simulation parameters and protocols, several parameters calculated from simulation can be compared to experimental observables.

The first report of atomistic MD simulations of bilayers containing fluorescent probes dates from 1997 and it was limited to a very short trajectory of less than 1 ns (López Cascales et al., 1997). Over the last decade, studies similar in principle but with much larger scope have focused on several important classes of probes (see Fig. 1 for structures).

Earlier works consisted mostly of atomistic simulations of simple nonpolar (and therefore easier to model) fluorophores in fluid disordered bilayers (easier to simulate). More recent studies have considerably widened the range of studied probes by simulating increasingly more complex fluorophores and extended the simulations to systems consisting of ordered bilayers, e.g. containing cholesterol (which adds considerable biological relevance, given the ubiquity of the latter in the plasma membranes of mammals (Gennis, 1989)). In addition, the recent introduction of coarse-grained force-fields in this field has allowed the study of much longer timescales and larger systems.

This chapter provides a review of this rapidly-evolving subject, which attempts to illustrate the wealth of detailed information that can be made available by these simulations, as well as to present the most recent trends in this field of research.

2. Atomistic simulations of membrane probes in lipid bilayers

2.1 Apolar fluorophores

Because of their relative structural simplicity, the first fluorescent probes simulated in lipid bilayers were small, apolar and highly symmetrical molecules, 1,6-diphenylhexatriene (DPH; Fig 1A) and pyrene (Fig. 1B).

2.1.1 DPH

DPH is a rod-shaped molecule whose fluorescence polarization is very sensitive to the microenvironment viscosity. Its fluorescence quantum yield and intensity decay show little sensitivity to the lipid phase, unlike the fluorescence anisotropy, which decreases threefold upon melting of the lipid acyl chains. For this reason, DPH is the archetypal membrane probe used for assessment of membrane fluidity (Lentz, 1989, 1993).

The most probable location of DPH inside the lipid bilayer was traditionally expected to be within the apolar acyl chain region, on account of its hydrophobicity. However, the question of its orientation remained unanswered for a long time. From analysis of time-resolved fluorescence anisotropy of the bilayer-inserted DPH, Litman and co-workers proposed a bimodal angular distribution of the long molecular axis, one of the two maxima corresponding to an alignment of this axis parallel to the membrane normal whereas the

other corresponded to a perpendicular alignment. Such a distribution is compatible with a location in the bilayer midplane, between the two monolayer leaflets (Straume & Litman, 1987; Mitchell & Litman, 1998). This perspective was challenged by an early report (López Cascales et al., 1997) of a pioneering MD simulation of a 72-molecule 1,2-dipalmitoyl-*sn*-3-glycerophosphocholine (DPPC) fluid bilayer in the presence of either one or three DPH molecules. No partial charges were used in any of the atoms of the DPH molecule and the temperature was set to 350 K, well above the main transition temperature of this phospholipid ($T_m=314$ K). However, this work was severely restricted by the extremely short time-scale probed (only ≤ 250 ps were used for analysis). In this study it was observed that the angle between the long molecular axis and the bilayer normal rarely was wider than 60° , and no perpendicular orientations were detected. Fast rotation motions (average correlation times of 0.061 ns for end-to-end tumbling and 0.0051 ns for the vector normal to the phenyl rings in the molecule) were obtained. An abnormally high DPH lateral diffusion coefficient ($1.36 \times 10^{-5} \text{ cm}^2\text{s}^{-1}$) resulted from this simulation. Significant disordering effects were observed for membranes containing DPH molecules, especially in the region closer to the lipid/water interface. In contrast, no significant probe effects were observed either in bilayer thickness or the area/lipid molecule.

A more conclusive study, employing larger (128-molecule) DPPC fluid bilayers ($T = 323$ K) labeled with 1 or 3 DPH molecules and simulated for a longer period of 50 ns, revealed broad angular distributions of the DPH long axis, and despite a peak being observed for $f(\theta)\sin(\theta)$ (where f is the orientation distribution function) at $\theta \approx 25^\circ$, significant distribution also occurs around $\theta \approx 90^\circ$ (Repáková et al., 2004). However, perpendicular orientations do not correlate with center of mass locations near the bilayer center. DPH was found to be located mostly deep in the acyl chain region of the bilayer, with its center of mass transverse position located in average at 0.75 nm from the bilayer center, in agreement with fluorescence quenching results (Kaiser & London, 1998). Two different approaches were adopted for attributing charges to DPH atoms, with largely identical results: zero charges on all atoms and partial charges obtained from *ab initio* quantum mechanical calculations. The extended time scale of this study enabled the authors to observe occasional probe translocation (flip-flop) events. Dynamic properties of DPH, such as lateral diffusion and rotational mobility, were also addressed. The correlation function for the long molecular axis had a relaxation time of 4.3 ns, which is in the same order of magnitude of the rotational correlation times measured by time-resolved fluorescence anisotropy. The calculated lateral diffusion coefficient of DPH ($20 \times 10^{-8} \text{ cm}^2\text{s}^{-1}$) was faster, albeit still in the same order of DPPC's ($15 \times 10^{-8} \text{ cm}^2\text{s}^{-1}$), possibly reflecting the increased free volume in the lipid acyl region of the bilayer.

A second part of this study (Repáková et al., 2005) focused on DPH effects on the properties of the host DPPC fluid bilayer (again 128 DPPC molecules; $T=323$ K) but simulation length was extended to 100 ns. The simulation was complemented with experimental differential scanning calorimetry (DSC) and deuterium nuclear magnetic resonance (^2H -NMR) measurements. DPH effects on the thermotropic phase behavior of DPPC were minor (very slight decrease of T_m , slight decrease in the corresponding transition enthalpy). ^2H -NMR data suggest that DPH has a very small orientating effect on the DPPC acyl chains. This was confirmed by the MD simulations, which were able to establish that, whereas this effect is indeed modest overall, significant increases in the calculated deuterium order parameter $-S_{\text{CD}}$ (up to 30–50%) were observed for lipid molecules in close proximity (<1.0 nm) of a

DPH molecule. Ordering effects become negligible for DPPC molecules separated from a DPH probe beyond a distance of 1.5 nm. Thus, by standing mostly upright in the membrane hydrophobic region, DPH produces a local ordering effect on fluid DPPC acyl chains. This is also apparent in the variation of the average area/lipid as a function of the distance to the nearest probe molecule. A ~2% overall decrease is observed, which is significantly more pronounced for DPPC molecules nearby a probe. Also consistent with this picture, there is a similar increase in bilayer thickness upon probe incorporation. DPH has negligible influence on interface properties such as membrane electrostatic potential and P-N tilt angles, but affects both lateral diffusion (halving the coefficient value) and rotation of the P-N axis (relaxation time increases by ~10%) for nearby DPPC molecules. Overall, it was concluded that DPH has a small perturbing effect on DPPC fluid bilayers justifying its wide use as a fluorescent membrane probe, though significant local ordering effects are observed.

More recently, the behavior of DPH was studied in bilayers composed of DPPC and cholesterol (with either 5 mol% or 20 mol% of the latter) (Franová et al., 2010). It was concluded that the increased order and membrane thickness resulting from the presence of cholesterol affects the location and orientation of bilayer-inserted DPH. The distance from the bilayer center to the average transverse location of DPH increased by 0.2 nm for the 20 mol% system, and the orientation distribution of the DPH long axis became narrower, with a single maximum for $\theta \approx 10^\circ$ and essentially zero values for $\theta \approx 90^\circ$. Similarly to the system without cholesterol, though detectable ordering effects were observed for the DPPC acyl chains closest to the DPH molecules, no significant overall perturbations were observed in parameters such as average area/lipid and deuterium order parameters. However, for the system with 20 mol% of cholesterol, the well-known ordering effect of this component is so dominant that the additional role of DPH becomes almost negligible. This paper also focused on a critical evaluation of the fluorophore orientations distribution study by time-resolved fluorescence anisotropy. The latter method allows the recovery of, at most, the first three coefficients ($\langle P_0 \rangle$, $\langle P_2 \rangle$ and $\langle P_4 \rangle$) of the Legendre polynomial series expansion of the orientational distribution function, whereas the complete function is readily available from MD simulation. It is shown that, whereas the truncation to the first three terms is still satisfactory for the more disordered systems (without cholesterol and with 5 mol%), important quantitative disagreement is observed for the cholesterol-rich ordered system.

2.1.2 Pyrene probes

Pyrene (Fig. 1B) is a polycyclic aromatic hydrocarbon which, both in free pyrene form and in pyrene-labeled lipids, has found a common use in membrane biophysics studies (Somerharju, 2002). This is due to its notable spectroscopic properties, including the unusually long fluorescence lifetime (>100 ns in a variety of solvents and membrane systems) and ability to form excimers.

Pyrene has been simulated by MD in 1-palmitoyl,2-oleoyl-*sn*-3-glycerophosphocholine (POPC) fluid bilayers (Hoff et al., 2005; this study combined MD and 2H-NMR measurements) and in both fluid and gel DPPC bilayers (Repáková et al., 2006; Čurdová et al., 2007). The former simulation study spanned 25 ns and the system consisted of 128 POPC molecules with four pyrene molecules inserted inside the membrane and a fifth located, at the start of the simulation, in the water region of the simulation box. The latter pyrene molecule was found to rapidly insert the POPC bilayer in less than 2 ns. Within ~8 ns of the

start, all five molecules were located slightly inside the headgroup region of the bilayer. This somewhat shallow location agrees with a published experimental fluorescence quenching report (Herrenbauer, 2002) and can be attributed to entropic effects. In fact, a considerable acyl-chain ordering and consequent decrease of entropy will result from the accommodation of this large, rigid molecule in the highly disordered middle region of the membrane. No flip-flops were observed in the time-scale of the simulation. The molecules were found to have their long axis essentially aligned (within $\pm 30^\circ$) with the bilayer normal. Good agreement between probe order parameter values determined from ^2H -NMR and from simulation was verified, seemingly indicating that even 25 ns of simulation seem to be enough to cover all types of motions that pyrene performs inside a lipid bilayer.

The two later studies focused both on probe properties and on its effect on the host bilayer. In the first (Repáková et al., 2006), 1, 4, and 6 molecules of the pyrene-tagged lipid 1-palmitoyl-2-(1-pyrenedecanoyl)-*sn*-glycero-3-phosphocholine (PyrPC) were simulated in a fluid ($T=323$ K) DPPC bilayer (128 total lipid molecules). In this study, no partial charges were used for the pyrene moiety. Although no significant overall effects were apparent in the average area/lipid molecule, sizeable reductions were detected locally for lipids within a range of 1.5 nm to the nearest PyrPC probe molecule. These effects were as high as $\sim 3\text{--}4\%$ for lipids closer than 1.0 nm. In accordance, increases in the calculated acyl chain's $-S_{\text{CD}}$ were apparent in the same range of distances. Interestingly, the area/PyrPC molecule was even smaller than that obtained for its nearest DPPC neighbors, and the $-S_{\text{CD}}$ value for the unlabeled *sn*-1 chain was notably high. This indicates that the pyrene moiety increases the order of both neighboring DPPC chains and also of the *sn*-1 chain of the lipid molecule to which it is attached. On the other hand, PyrPC incorporation had very minor effects on the DPPC density profiles or bilayer thickness. The label was mostly found ~ 0.8 nm from the lipid/water interface, in the hydrocarbon region of the bilayer. The fluorophore adopted a broad distribution of orientations, implying a significant fraction of pyrene labels pointing towards the water-lipid interface, causing a kink in the probe's *sn*-2 acyl chain. For molecules that did not present this behavior, the pyrene group often interdigitated to the opposite leaflet ($\sim 3\text{--}6\%$ of all configurations). According to the authors, this behavior can cause occasional excimer formation involving PyrPC molecules of different leaflets. Another interesting consequence of pyrene interdigitation was an increase in $-S_{\text{CD}}$ of the nearest ($R < 0.5$ nm) DPPC acyl chains in the other leaflet.

The second study (Čurdová et al., 2007) concerned free pyrene, in both fluid (0:128, 1:128, and 3:128 pyrene/lipid ratios, $T=325$ K or 350 K, $t=20$ ns) and gel (0:120, 1:120, and 3:120 pyrene/lipid ratios, $T=273$ K, $t=50$ ns) DPPC bilayers. Partial charges of pyrene atoms were obtained from *ab initio* quantum mechanical calculations. In similarity with the previous PyrPC studies, the overall effects of pyrene on area/lipid and $-S_{\text{CD}}$ were minor for all systems. However, significant local (for lipids at less than 1.0 nm from the probe) effects were present. In the fluid phase simulations, acyl chain ordering similar to that described for PyrPC above was observed. Concerning the gel phase, the fraction of *trans/gauche* defects along the acyl chains of neighboring DPPC molecules increased, meaning pyrene molecules decreased their ordering. However, the presence of pyrene also induced a reduction in the tilt angle of nearby DPPC acyl chains, which would *per se* result in an increased order parameter (as the latter reflects the angle between the chain and the bilayer normal). It is, thus, difficult to make an analysis of $-S_{\text{CD}}$ in face of these contradictory effects. Pyrene

incorporation caused a significant reduction and a minor increase of the bilayer thickness in the gel and fluid phases, respectively. This probe presented broad transverse distribution and orientation profiles, with maxima around phospholipid acyl chain carbon 5 (in terms of the transverse distribution) and for $\theta=90^\circ$ (corresponding to the normal of the pyrene plane being perpendicular to the membrane normal direction), respectively. Both observations are in agreement with Hoff et al. (2005). In the gel phase, the orientation profile is slightly more complex, with a second maximum being apparent at 50° (probably reflecting the tilt of the DPPC acyl chains). No significant changes in the lateral diffusion coefficient of DPPC were observed upon pyrene insertion. No clustering of pyrene molecules was observed, possibly as a result of time scale limitations.

Similarly to the effects reported by Čurdová et al. (2007) in DPPC gel, recent unpublished data by Loura and Do Canto regarding simulations of pyrene in 80% POPC:20% cholesterol mixed bilayers (see snapshot in Fig. 2) showed that pyrene produces a disordering effect, increasing the area/lipid molecule and decreasing the bilayer thickness and acyl chain order parameter, and thus opposing the ordering effect of cholesterol. Although the overall variations of these parameters were modest, significant local effects were apparent (Fig. 3). This observation is in contrast to that of DPH in DPPC/cholesterol 4:1 (Franová et al., 2010), for which a slight ordering effect was reported, as described above. The difference in behavior of the two probes is probably due to pyrene being substantially bulkier and therefore more difficult to accommodate in an ordered bilayer without inducing perturbation.

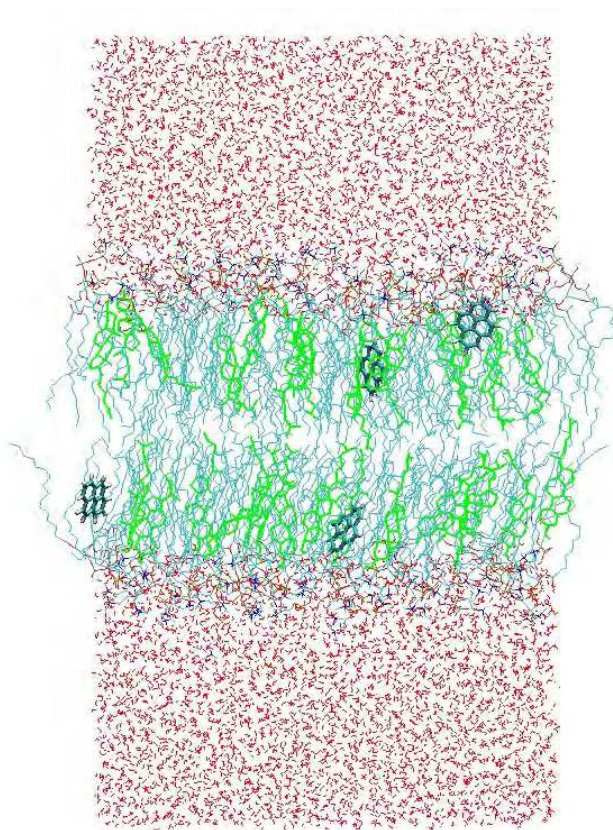


Fig. 2. Snapshot of a POPC/cholesterol 4:1 bilayer containing 4 pyrene molecules.

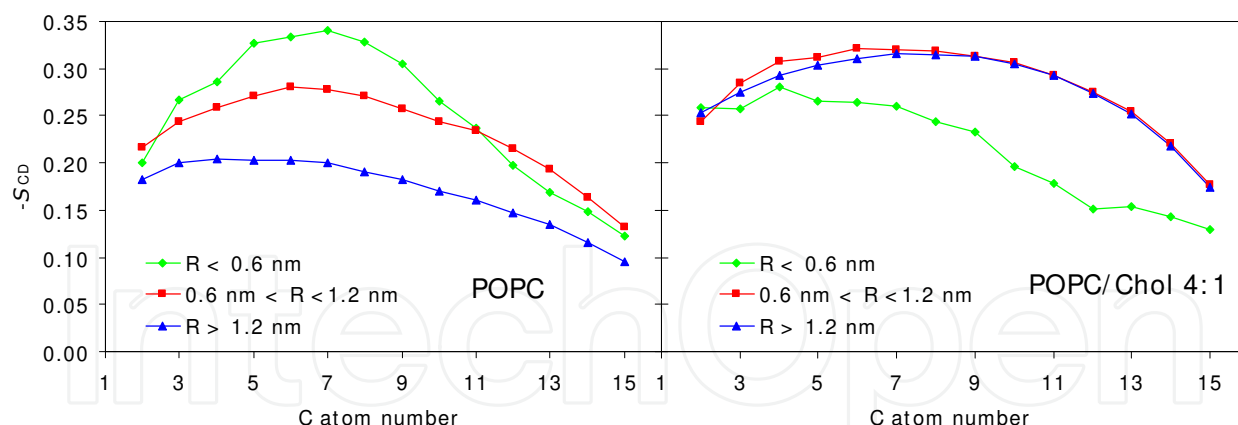


Fig. 3. Deuterium order parameter profile of the POPC *sn*-1 chain for varying proximity to the closest pyrene molecule (R) in the 100-ns MD simulation of (a) POPC/pyrene (128:2) and (b) POPC/cholesterol/pyrene (120:30:2) bilayers. For $R > 1.2$ nm, the profiles are essentially identical to those obtained in absence of probe in both systems (not shown). Significant local ordering is observed for $R < 1.2$ nm in (a), whereas significant local disordering is observed for $R < 0.6$ nm in (b).

2.2 Polar fluorophores

The use of fluorescent membrane probes bearing polar design fluorophores has become very common, especially since the 1980s. Despite having arrived later to the scene, MD simulations of this type of fluorophores are currently outnumbering those involving apolar fluorescent membrane probes.

2.2.1 NBD probes

Among polar fluorophores, a popular family is that of phospholipids labeled with the 7-nitrobenz-2-oxa-1,3-diazol-4-yl (NBD) fluorophore in one of the acyl chains. NBD derivatives are commercially available for all major phospholipid classes, and have been used extensively as fluorescent analogues of native lipids in biological and model membranes to study a variety of processes (Chattopadhyay, 1990; Mukherjee et al., 2004).

Simulations of two of these probes, the acyl chain-labeled phosphatidylcholine derivatives 1-palmitoyl,2-{6-[(7-nitro-2,1,3-benzoxadiazol-4-yl)amino]hexanoyl}-*sn*-glycero-3-phosphocholine (C6-NBD-PC) and 1-palmitoyl,2-{12-[(7-nitro-2,1,3-benzoxadiazol-4-yl)amino]dodecanoyl}-*sn*-glycero-3-phosphocholine (C12-NBD-PC; Fig. 1C), in fluid DPPC bilayers (0:64, 1:63, 4:60 NBD-PC/DPPC bilayers, $T=323$ K, $t=100$ ns) have been reported in two complementary studies. The first one addressed primarily the locations and dynamics of the probes (Loura & Prates Ramalho, 2007) whereas the second focused on their effects on the host bilayer properties (Loura et al., 2008). Parameterization of the NBD moiety required energy minimization for geometry and *ab initio* quantum mechanical calculations for partial atomic charges. Simulations were complemented with time-resolved fluorescence anisotropy (Loura & Prates Ramalho, 2007) and DSC (Loura et al., 2008) measurements, which provided experimental information on probe rotational dynamics and perturbation of the thermotropic behavior of DPPC bilayers, respectively. In these two studies it was

observed that NBD fluorophores loop in the direction of the interface. The transversal distribution across the bilayer has a broad profile, with a maximum around the glycerol backbone/carbonyl region, in accordance with fluorescence quenching and ^2H -NMR results (Chattopadhyay & London 1987; Huster et al., 2001), and with the nitro group being closest to the interface. It was also observed that the NBD's NH group is involved in H-bonding to PC glycerol backbone O atoms. In terms of the dynamical behavior, the calculated lateral translation diffusion of NBD-PC was found to be identical to that of DPPC and the theoretical rotational dynamics of NBD agreed well with experimental fluorescence anisotropy decays. Whereas important effects were observed for high (~6 mol%) probe content, milder perturbation of fluid PC structure and dynamics is expected for ~1 mol% or lower amounts of probe (the concentrations most frequently used in experimental work). Regarding the range of the induced perturbations, as judged by $-S_{\text{CD}}$ values, they occur mostly in molecules in close contact with probes. This is especially true for C6-NBD-PC. Because the labeled *sn*-2 chain of this probe does not extend nearly so much across the bilayer as that of C12-NBD-PC, the disordering effect of the former is mostly concentrated in its immediate vicinity, whereas the large extension of the C12-NBD-PC *sn*-2 chain allows for a more uniform distribution of the perturbation among additional layers of neighbors. Because most fluorescence parameters are dictated by the immediate environment of the chromophore, this implies that C12-NBD-PC may be considered a better reporter of membrane properties than C6-NBD-PC. However, even for these smaller amounts, large alterations (transition temperature shifts, loss of cooperativity), are evident in the thermotropic behavior of NBD-PC labeled PC bilayers, as measured by differential DSC.

These 100-ns simulations of NBD-PC in fluid DPPC were also used in a later study to calculate the FRET orientation factor (κ^2) for homo-FRET between these probes embedded in this membrane system (Loura et al., 2010a). κ^2 is a measure of the relative orientation of FRET donor and acceptor transition dipoles and can be calculated according to van der Meer et al. (1994):

$$\kappa^2 = (\cos \theta_T - 3 \cos \theta_D \cos \theta_A)^2 \quad (1)$$

where θ_T is the angle between the transition moments of the donor and acceptor and θ_D and θ_A are the angles between the donor and acceptor transition moments and the vector uniting their centres (see Loura et al, 2010a for details). κ^2 can vary between 0 (corresponding to several dipole arrangements) and 4 (collinear dipoles). The value of κ^2 is required for calculating the characteristic distance for the FRET interaction, the so-called Förster radius R_0 as seen in e.g. van der Meer et al. (1994):

$$R_0^6 = \frac{9000(\ln 10)\kappa^2 Q_D J}{128\pi^5 n^4 N_{\text{AV}}} \quad (2)$$

where Q_D is the quantum yield of the donor in the absence of any acceptor molecules, n is the refraction index of the medium, N_{AV} is the Avogadro number and J is the normalized overlap integral between the donor emission and the acceptor absorption spectrum.

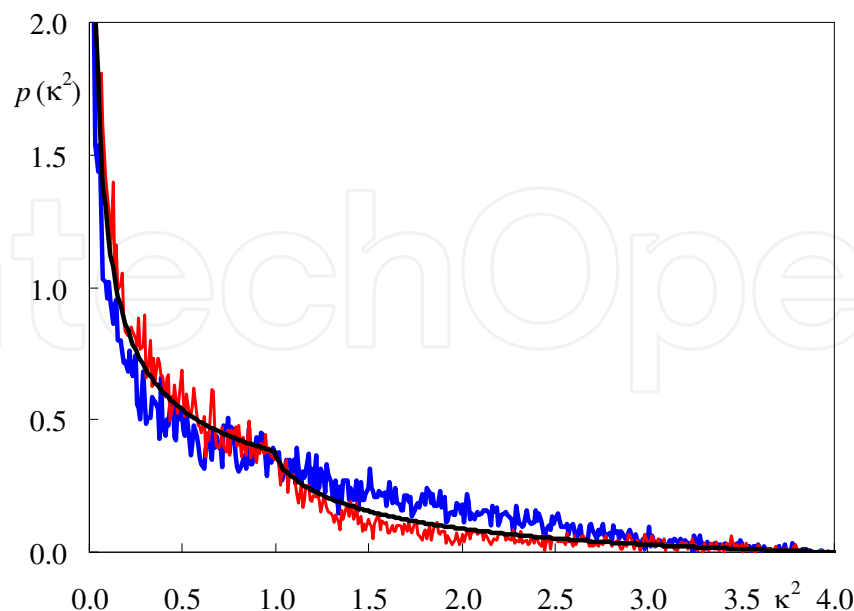


Fig. 4. Calculated probability density $p(\kappa^2)$ for C6-NBD-PC (red) and C12-NBD-PC (blue), compared with the analytical isotropic result of Eq. 3 (black).

R_0 is an essential parameter for the quantitative description of FRET kinetics in membrane systems (Loura et al., 2010b, 2010c) as well as in the classic use of FRET as a spectroscopic ruler (Stryer, 1978). In the preceding equation, whereas Q_D and J may be obtained from straightforward calculations from spectral data, there is no experimental technique suited to a definite measurement of κ^2 (though it was shown by Dale and co-workers (1979) that intervals containing its average value $\langle \kappa^2 \rangle$ can be inferred from adequate fluorescence anisotropy measurements). Most often, the theoretical value for the so-called dynamic isotropic limit ($\langle \kappa^2 \rangle = 2/3$) is used, but the uncertainty in the value of $\langle \kappa^2 \rangle$ is still widely regarded as an inconvenience that may be especially important in membranes, because of their intrinsic anisotropic nature and the restricted rotational mobility experienced by fluorophores incorporated inside the bilayer. However, from the position coordinates in an MD trajectory the calculation of κ^2 for a given FRET donor-acceptor molecular pair is straightforward, and averaging both over pairs and over time is conveniently carried out. Fig. 4 shows the probability densities of κ^2 for the C6-NBD-PC and C12-NBD-PC systems, compared with the theoretical isotropic orientation result which is given by Eq. 3 (van der Meer et al., 1994):

$$p(\kappa^2) = \begin{cases} \frac{1}{2\sqrt{3}\kappa^2} \ln(2 + \sqrt{3}) & 0 \leq \kappa^2 \leq 1 \\ \frac{1}{2\sqrt{3}\kappa^2} \ln\left(\frac{2 + \sqrt{3}}{\sqrt{\kappa^2} + \sqrt{\kappa^2 - 1}}\right) & 1 \leq \kappa^2 \leq 4 \end{cases} \quad (3)$$

Although the distributions generally resemble the analytical solutions for isotropic dipoles, $\langle \kappa^2 \rangle$ for C12-NBD-PC (0.87 ± 0.06) is $\sim 30\%$ higher than the $2/3$ dynamic isotropic limit, whereas $\langle \kappa^2 \rangle$ for C6-NBD-PC (0.61 ± 0.03) is slightly lower than that limiting value. These

values are discussed in the original reference in terms of preferential orientation of the NBD group approximately parallel to the bilayer plane, as well as some extent of probe aggregation in the case of C6-NBD-PC. To our knowledge, this was the first calculation of κ^2 for intermolecular FRET by atomistic molecular simulation methods. A previous study, limited to a 100-ps timescale, focused in intramolecular FRET occurring in a non-membrane dye (Harriman et al., 2006). This methodology provides a way to calculate R_0 with improved accuracy relative to the widespread $\langle \kappa^2 \rangle = 2/3$ assumption, and can also be employed in hetero-FRET κ^2 calculation, provided that bilayers containing both donor and acceptor probes are simulated.

Other NBD membrane probes are currently being studied by MD simulations, including the homologous series of fatty amines NBD- C_n (Filipe et al. 2011), the head-labeled phospholipid 1,2-dipalmitoyl-*sn*-glycero-3-phosphoethanolamine-*N*-(7-nitro-2-1,3-benzoxadiazol-4-yl) (NBD-PE) and some NBD-labeled analogs of cholesterol, namely the 22-(*N*-(7-nitrobenz-2-oxa-1,3-diazol-4-yl)amino)-23,24-bisnor-5-cholen-3 β -ol (22-NBD-Cholesterol; Fig. 1D) and the 25-[*N*-[(7-nitro-2-1,3-benzoxadiazol-4-yl)methyl]amino]-27-norcholesterol (25-NBD-Cholesterol; Fig. 1E). Regarding the latter NBD-cholesterol probes, they are among the commercially available fluorescent analogs of cholesterol. This sterol is a major component of mammalian cell membranes, and its action upon the physical properties of lipid bilayers has been studied actively in the last four decades. More recently, its implication in raft domains (Simons & Ikonen, 1997) has further increased this interest. Although both 22- and 25-NBD-cholesterol have been used for characterizing the distribution and dynamics of cholesterol in several systems (for a recent review, see e.g. Gimpl & Gehrig-Burger, 2011), the location and orientation of the NBD group of these probes in lipid bilayers is still a controversial issue. Using time-resolved fluorescence, it has been shown that 22-NBD-cholesterol preferably distributes to the cholesterol-poor liquid disordered (ld) phase rather than to the cholesterol-rich liquid ordered (lo) phase in phase separated PC/cholesterol vesicles (Loura et al., 2001). This displacement from the cholesterol-enriched phase is obviously an anomalous behavior for a probe supposed to mimic the behavior of the cholesterol component. From fluorescence quenching, it was found that the fluorophore of 25-NBD-cholesterol was deeply buried within the bilayer (Chattopadhyay & London, 1987). In contrast, using NMR, it was observed that both NBD-sterols may adopt an upside-down orientation within bilayers (Scheidt et al., 2003). This discrepancy remains unsolved in the literature. The technique of MD simulations is well suited to clarify this question, and both sterols have very recently been simulated in POPC bilayers (Loura & Prates Ramalho, unpublished data). Although complete trajectory analysis is still underway, it is clear from the structures obtained after 100 ns simulation (Fig. 5) that both sterols adopt a conformation where both opposing polar groups (-OH and -NO₂) are simultaneously oriented towards the interface. This behavior is at odds with the well-known orientation of cholesterol, with the hydroxyl group towards the interface, and the long axis approximately perpendicular to the bilayer plane (Franks, 1976; Worcester & Franks, 1976). Therefore, this study seems to confirm that both 22- and 25- NBD-cholesterol are inappropriate cholesterol analogs, probably at variance with BODIPY-cholesterol (see section further ahead), whose orientation in the bilayer resembles that of cholesterol (Hölttä-Vuori et al., 2008).

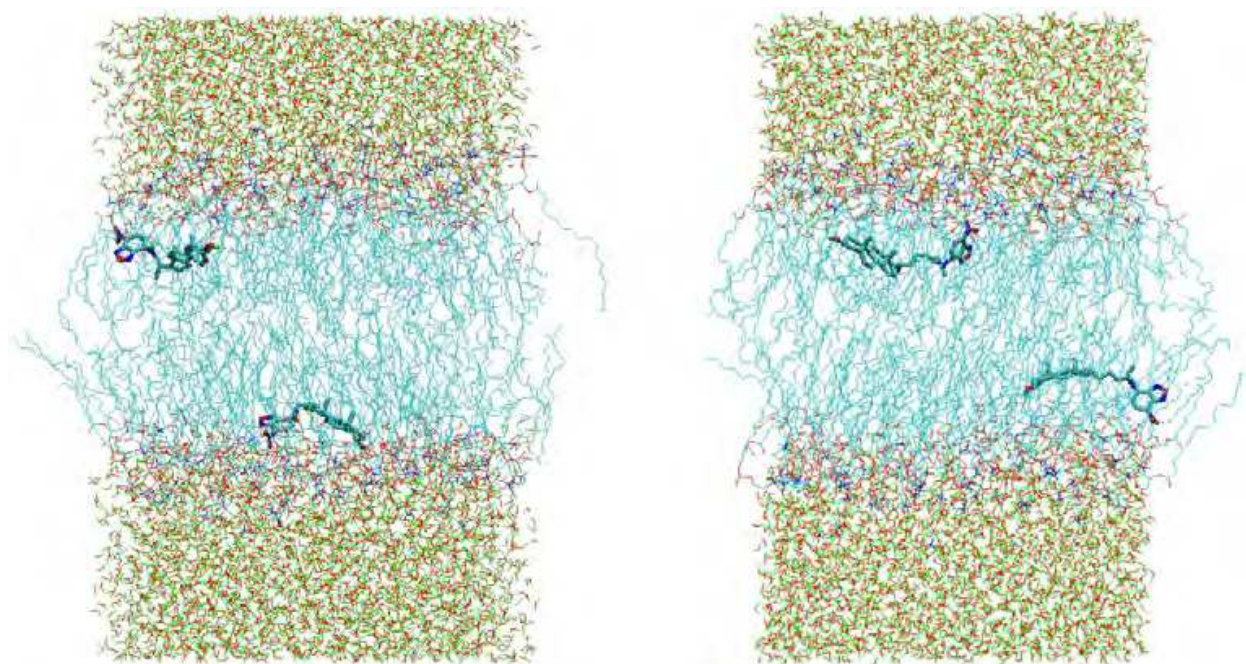


Fig. 5. Final snapshots of 100-ns MD simulations of fully hydrated 128-molecule fluid POPC bilayers with either two 22-NBD-cholesterol (left) or two 25-NBD-cholesterol (right) molecules inserted.

2.2.2 DiI

1,1'-dioctadecyl-3,3',3',3'-tetramethylindocarbocyanine (DiI_{C18}(3) or DiI; Fig. 1F) is the most representative member of the carbocyanine family of dyes. These molecules have very high molar absorption coefficients ($\sim 10^5 \text{ M}^{-1} \text{ cm}^{-1}$) and are used as membrane potential probes and as stains in cell studies. They have also been extensively used as probes of bilayer dynamics and structure (Wolf 1988). MD simulations have been performed by Gullapalli et al. (2008) to study the behavior of DiI in fluid DPPC bilayers. The simulated systems consisted of 0:128, 2:126, and 4:124 DiI/DPPC bilayers, at a temperature of 323 K, for a simulation length of 40 ns in each case. Partial atom charges on the DiI headgroup (global charge +1) were obtained from *ab initio* quantum mechanical calculations. A fourth simulation, similar to the 4:124 case, but in the absence of any partial charges on the DiI head group, was also performed for the sake of comparison.

It was found that, whereas DiI does not affect the area/lipid molecule significantly, membrane thickness was found to increase by 3–5% ($\sim 0.1\text{--}0.2$ nm) in presence of the incorporated probe. In accordance, DiI was found to induce an increase in $-S_{\text{CD}}$ for both *sn*-1 and *sn*-2 DPPC acyl chains. The center of mass of the DiI headgroup was distributed from a distance of 0.3 to 2 nm from the center of the bilayer, with a maximum at 1.26 nm, in the glycerol/upper acyl chain region, and below the phospholipid headgroup region. As pointed out by the authors, this result is in contrast to some popular cartoon representations of DiI but consistent with DiI's increase in fluorescence quantum yield when incorporated into lipid bilayers. Flip-flop was observed in the control simulation with uncharged DiI atoms but not in the other simulation runs, indicating that the overall positive charge prevents the occurrence of probe translocation. The angle between the chromophore long

axis (uniting the two C6 rings) and the bilayer normal had a broad average distribution, with a maximum at 77° , almost parallel to the bilayer plane, in accordance with fluorescence polarization data (Axelrod 1979). Addition of DiI leads to an ordering of the water at the interfacial region (mainly as a consequence of the increase in the bilayer's thickness), decrease in the angle between the P-N vector and the bilayer normal, and a significant variation of the electrostatic potential across the membrane from -0.56 V (DPPC) to -0.69 V (4 DiI:124 DPPC). The latter values can be compared with the above described NBD study (Loura et al., 2008) for which a smaller variation was observed for higher labeling ratios (-0.55 V for DPPC, -0.58 V for 4 C6-NBD-PC:60 DPPC, -0.64 V for 4 C12-NBD-PC:60 DPPC). The decay of the autocorrelation function of the chromophore axis agrees with literature anisotropy decay parameters of related carbocyanines, and DiI has a lateral diffusion coefficient identical to that of DPPC.

2.2.3 BODIPY probes

Recently, a cholesterol derivative bearing the 4,4-difluoro-4-bora-3a,4a-diaza-s-indacene (boron-dipyrromethene, BODIPY) fluorophore (BODIPY-cholesterol; see Fig. 1G) was found to partition into ordered domains in model membranes (Shaw et al., 2006). A recent work using BODIPY-cholesterol combined live cell imaging (which established that the probe closely mimics the membrane partitioning and trafficking of cholesterol) with MD simulations (Hölttä-Vuori et al., 2008). Focusing on the latter, systems with both DPPC and *N*-palmitoylsphingomyelin (SM) at $T=323$ K, were simulated for a duration of ≥ 60 ns in each case. In a first set of simulations (3.125% sterol), the bilayers were composed of 124 DPPC or SM molecules and 4 sterol molecules. The used sterol was either cholesterol or BODIPY-cholesterol. In a second set (20% total sterol), bilayers of 128 SM or DPPC and 32 cholesterol molecules were simulated, as well as bilayers with 128 SM or DPPC, 28 cholesterol and 4 BODIPY-cholesterol molecules. Since the BODIPY moiety contains a boron atom, and this atom type was not originally included in the used force field, this had to be adapted for the purpose. Partial atom charges in the fluorophore were obtained from *ab initio* quantum mechanical calculations. It was found that the effects of BODIPY-cholesterol on bilayer properties matched those of cholesterol. Differences in the effect of sterol upon the area/lipid and the membrane thickness were not significant. Differences upon $-S_{CD}$, while noticeable, were relatively minor (BODIPY-cholesterol was slightly less efficient in ordering fluid lipid acyl chains than cholesterol; for both molecules the perturbation extended over a range in the order of ~ 1.0 nm). The distribution of the angle between the vector uniting the ends of the sterol ring system and the bilayer normal showed a predominance of small angles ($<45^\circ$) in all cases. Distributions of BODIPY-cholesterol were slightly wider and displaced to larger angles as compared to those of cholesterol. On the other hand, the angle between the longer axis of the BODIPY moiety itself and the bilayer is predominantly at $>45^\circ$. Given that the maximum of the mass distribution profile of the BODIPY moiety is in the middle of the bilayer, one can expect to find the probe molecules with their chromophore located deep along the bilayer midplane. This is the predominant configuration, corresponding to an upright orientation of the steroid ring system (similar to cholesterol); for low sterol bilayers, a significant probe population displays a more tilted steroid ring system, together with a slight upwards loop of the BODIPY moiety.

Remarkably, in more ordered bilayers (containing SM instead of DPPC, or 20 mol% sterol instead of 3.125%), this second population tends to vanish, giving rise to unimodal orientation distributions of BODIPY-cholesterol, as the lipid acyl chains become more ordered. This means that BODIPY-cholesterol is an especially good mimic of cholesterol for more ordered environments, which is an important asset for a raft reporter. The location and orientation of cholesterol itself is not affected by the presence of a smaller amount of BODIPY-cholesterol.

Very recently, a BODIPY-acyl-chain labeled phospholipid probe (2-(5-butyl-4,4-difluoro-4-bora-3a,4a-diaza-s-indacene-3-nonanoyl)-1-hexadecanoyl-*sn*-glycero-3-phosphocholine; see Fig. 1H) was simulated in DPPC monolayers and bilayers in the NPAT (constant pressure, area, and temperature) ensemble (Song et al. 2011). Three area/lipid molecule values were explored, 0.77 nm², 0.64 nm² and 0.40 nm², corresponding to lateral pressures of 5 mN/m, 10 mN/m and 40 mN/m, respectively. From the density profiles it was observed that the BODIPY moiety resided in the hydrophobic region of the bilayer. The calculated distributions of the tilt of BODIPY fluorophore long axis revealed ordering (shifting to narrower distributions, closer to the orientation of the bilayer normal) upon increasing lateral pressure. In any case, even for low and medium lateral pressure, the tilt angle was mostly < 90°, indicating that snorkeling of BODIPY, while permitted for these lower pressure values, is not predominant. However, the calculated tilt distributions do not agree with the bimodal histograms obtained from analysis of single molecule orientation measurements carried out in a total internal reflection fluorescence microscope. These experimental distributions were consistent with two fluorophore orientations, one normal and another parallel to the membrane plane. In any case, these simulations reinforce the notion that BODIPY might be a better behaved fluorophore (compared to NBD) for reporting the hydrophobic region of membranes.

2.2.4 Headgroup-labeled phospholipid probes

Given the significant degree of perturbation induced by phospholipids labeled at the acyl chain with polar fluorophores (as evidenced by the NBD-PC studies described above), it would be reasonable to assume that headgroup-labeled lipid probes present a potentially less membrane-disturbing behavior. This hypothesis can be tested using MD simulations. Two recent reports address specifically the behavior of phospholipids labeled at the headgroup with rhodamine dyes in fluid DPPC bilayers. Skaug et al. (2009) simulated Texas Red-1,2-dihexadecanoyl-*sn*-glycero-3-phosphoethanolamine (TR-DHPE; Fig. 1I), whereas Kyrychenko (2010a) simulated 1,2-dipalmitoyl-*sn*-glycero-3-phosphoethanolamine-*N*-(lissamine rhodamine B sulfonyl) (Rhod-DPPE; Fig. 1J). As seen from the structures, these probes share an identical phosphatidylethanolamine lipid moiety and present quite similar fluorophores attached to the headgroup. In both cases, fluorophore parameterization involved density functional theory (DFT) quantum mechanical calculations. Although the two fluorophores have similar structures, higher absolute charges were consistently obtained for the Rhod-DPPE case, possibly due to differences in the methodology and details of the two DFT calculations. Perhaps for this reason, the two studies predict different transverse locations for the two fluorophores at equilibrium, with Texas Red in the upper acyl chain region and lissamine rhodamine B sulfonyl in a more external position, near the water/lipid interface (co-localizing with the phosphate and choline groups of DPPC). This

different behavior is not consistent with parallax analysis of experimental fluorescence quenching results, which predicts identical transverse locations of the two fluorophores in 1,2-dioleoyl-*sn*-glycero-3-phosphocholine vesicles (Kachel et al., 1998), despite TR being slightly more hydrophobic than lissamine rhodamine B sulfonyl. The distinct behaviors of the two simulated probes therefore possibly stem from the differences in the model building procedure, which emphasizes the importance of careful parameterization of these polar fluorophores. It could be argued that the combination of different starting positions and incomplete equilibration would be another possible cause for this difference. In fact, the fluorophore of Rhod-DPPE was located outside the headgroup region (into the water region) in the starting structure (Kyrychenko, 2010a), whereas that of TR-DHPE appears to have been placed inside the DPPC headgroups (Skaug et al., 2009). However, both articles report convergence of both average area/lipid and fluorophore transverse position, thus invoking effective equilibration.

In the study by Skaug et al. (2009), both 1 TR-DHPE:127 DPPC and 1 TR-DHPE:511 DPPC systems were simulated, with slightly different fluorophore transverse locations and orientations being obtained from the two simulations. As expected from its location, the bulky Texas Red fluorophore introduces local disordering in the DPPC acyl chains which is apparent from the decrease of $-S_{CD}$ (in both systems) and the increase in the average area/lipid values (in the 1 TR-DHPE:127 DPPC system only) for the DPPC molecules closest to the probe. It was observed that the aryl group of Texas Red and the P atom of a particular DPPC lipid remained in close contact (≈ 0.5 nm of each other) throughout the duration of both 1 TR-DHPE:127 DPPC and 1 TR-DHPE:511 DPPC simulations (Skaug et al., 2009). On the other hand, the core of the fluorophore of Rhod-DPPE presented a tilt of $44^\circ \pm 8^\circ$ relative to the bilayer normal, and 2 Rhod-DPPE:126 DPPC bilayers showed reduced (by $\sim 5\text{-}10\%$) $-S_{CD}$ values in all positions of the DPPC acyl chains (Kyrychenko, 2010a). On the whole, a significantly smaller degree of probe perturbation induced by headgroup-labeled lipid probes, compared to acyl-chain labeled lipid probes, could not be verified, as both studies report disordering effects of probe incorporation on the bilayer structure. Especially important effects were recently described in 500 ns simulations of a 24 TR-DHPE:488 DPPC (5 mol%) bilayer (Skaug et al., 2011). These included significant orientation distribution changes, clearly distinct lateral diffusion dynamics of host lipid and probe, and a predicted perturbation of the liquid ordered/liquid disordered phase diagram of a ternary saturated lipid/unsaturated lipid/cholesterol mixture upon incorporation of 1 mol% TR-DHPE.

Whereas the above studies concerned commercially available fluorescent membrane probes that have found previous use in the membrane fluorescence research community, recent works combined fluorescence measurements and MD simulations to address the behaviour of novel environment-sensitive 2-(2'-Pyridyl)- and 2-(2'-Pyrimidyl)-Indoles (Kyrychenko et al., 2010b) and 2,6-bis(1*H*-benzimidazol-2-yl)pyridine (Kyrychenko et al., 2011) in POPC. Spectral shifts and variation of steady-state and time-resolved fluorescence in different environments were measured, and in MD simulations several parameters were calculated, including the kinetics of insertion into the bilayer from the water region, the equilibrium transverse location, the inserted probes' orientations, hydrogen bonding involving water and probe molecules, and the free energy profile of penetration (estimated using the method of potential of mean constraint force (PMF)). From the latter, free energies of probe insertion were calculated that agreed well with the experimental values obtained from fluorescence intensity variation upon titration with lipid vesicles.

3. Coarse-grained simulations of dyes in lipid bilayers

Coarse-grained models represent molecules in a simplified way, e.g. by combining multiple atoms into a single interaction site or bead. This allows the simulation of larger systems for longer times than that sampled in more detailed atomistic simulations. However, this is achieved at the expense of atomic resolution, which is generally critical to many of the aspects that are commonly studied in MD simulation of fluorophores. One sole coarse-grained study of a fluorescent membrane probe (voltage sensitive dye dibutyl-amino-styryl-pyridinium-butyl-sulfonate or Di-4-ASPBS; Fig. 1K) and its derivatives interacting with POPC bilayers has been reported (Hinner et al., 2009), using the MARTINI forcefield (Marrink et al., 2007). In this work, coarse-grain simulations were used to compute the free energy of binding of these dyes to the bilayer. The determination of this parameter from atomistic simulations is highly demanding from the numerical point of view, and coarse-grained methodologies allow its calculation at a fraction of the computational cost. Validation of the MARTINI simulations was achieved by calculation of the fluorophore transverse position and orientation, and the successful comparison with atomistic simulations and experimental data. Constraint options were optimized for the determination of the PMF using umbrella sampling, in order to sample conveniently the water/membrane partition (at the expense of an adequate sampling of flip-flop motions).

Although the study was generally successful, the effects of increasing the lipophilic tail chain length and introducing polar phosphoric acid ester groups at the head or tail of these amphiphiles on the free energy of membrane binding were only semiquantitatively reproduced. Most importantly, the authors observed an overestimation of the free energy increase with increasing chain length of the Di-4-ASPBS derivatives. The underlying reasons for this effect were not clear, as the increment in binding free energy, calculated for a series of alcohols using the same parameterization and simulation protocols, was in agreement with experiment. A possible explanation is that the experimental data might be biased due to dye aggregation in the aqueous phase, especially for the longer-chained derivatives (for which discrepancies are larger). In any case, this study showed that calculation of the partition of membrane-active molecules from careful coarse-grained MD simulations is both fast and sufficiently accurate to provide a useful tool in computational membrane biophysics.

4. Concluding remarks

MD simulations of fluorescence membrane probes interacting with lipid bilayers are still somewhat scarce, but the last few years have seen a dramatic increase and diversification of the use of MD simulations to study the behavior of these systems, indicating that this is fast becoming a very active field within theoretical modeling of membranes. The possibilities offered by this approach are clearly visible from the studies described in this review. Validation of the methodology has frequently been achieved through the verification of several experimental observables. Most importantly, unique information has been retrieved, both on probe properties and regarding their effect on the host bilayer. The combination of simulation of the probes' behavior and experiments designed taking this behavior into consideration has potential to provide accurate insights on membrane structure and function at a molecular level.

Simulation work initially focused in simpler apolar fluorophores (such as DPH or pyrene) in liquid disordered bilayers. Such earlier studies served to show that many of the reported effects of probes in fluid lipid bilayers are minor and most noticeable for lipid molecules close to a probe or for high probe concentration. Recent emphasis has been gradually shifting to more complex design polar fluorophores such as NBD, BODIPY, rhodamine or cyanine groups. The number of studies addressing this type of probes has clearly surpassed those dealing with the traditional small lipophilic compounds during the last two years. Furthermore, simulations of lipid bilayers in liquid ordered and gel phases are also becoming more frequent, which reflects the recognized importance of ordered and even rigid domains such as lipid rafts (Simons and Ikonen, 1997) and ceramide platforms (Zhang et al., 2009), where the problem of finding adequate fluorescent reporters is more critical.

The increase in complexity of the simulated systems has highlighted the importance of adequate parameterization. Methodological differences in parameterization may produce substantially divergent results, as illustrated in the above comparison of the two studies of structurally very similar rhodamine headgroup-labeled phospholipids. For this reason, careful testing against experimentally well-characterized systems is still required.

Recently, the free energy of probe partition into the bilayer was added to the list of calculated parameters. The determination of the extent of interaction of a given compound with bilayers is usually the first step in the characterization of its behavior in membranes. Unless the amounts of compound in the water and lipid media are known, experimental quantitative characterization of many parameters is not feasible. To this effect, determination of PMF using umbrella sampling is an approach made available from MD simulations. Theoretical calculation of the free energy of bilayer partition is particularly advantageous for prediction purposes, as well as in situations where experimental determination is difficult e.g. due to probe aggregation or limited solubility in the aqueous medium. As illustrated by the above described works, where atomistic simulations are too demanding for the size and complexity of the systems of interest, coarse-grained simulations may provide an attractive alternative as they allow for much faster computation. For many parameters, however, atomic resolution is generally essential, and atomistic simulations remain the method of choice.

5. Acknowledgments

We acknowledge support by Fundação para a Ciência e Tecnologia (Portugal) through project PTDC/QUI-QUI/098198/2008, co-funded by FEDER (program FCOMP-01-0124-FEDER-010787).

6. References

- Ash WL, Zlomislic MR, Oloo EO, Tieleman DP (2004) Computer simulations of membrane proteins. *Biochim Biophys Acta* 1666:158–189, ISSN 0006-3002
- Axelrod D (1979) Carbocyanine dye orientation in red cell membrane studied by microscopic fluorescence polarization. *Biophys J* 26:557–573, ISSN 0006-3495
- Berkowitz ML (2009) Detailed molecular dynamics simulations of model biological membranes containing cholesterol. *Biochim Biophys Acta* 1788:86–96, ISSN 0006-3002

- Bouvrais H, Pott T, Bagatolli LA, Ipsen JH, Méléard P (2010) Impact of membrane-anchored fluorescent probes on the mechanical properties of lipid bilayers. *Biochim Biophys Acta* 1798:1333-1337, ISSN 0006-3002
- Chattopadhyay A (1990) Chemistry and biology of N-(7-nitrobenz-2-oxa-1, 3-diazol-4-yl)-labeled lipids: fluorescent probes of biological and model membranes. *Chem Phys Lipids* 53:1-15, ISSN 0009-3084
- Chattopadhyay A, London E (1987) Parallax method for direct measurement of membrane penetration depth utilizing fluorescence quenching by spin-labeled phospholipids. *Biochemistry* 26:39-45, ISSN 0006-2960
- Čurdová J, Čapková P, Plášek J, Repáková J, Vattulainen I (2007) Free pyrene probes in gel and fluid membranes: perspective through atomistic simulations. *J Phys Chem B* 111:3640-3650, ISSN 1520-6106
- Dale RE, Eisinger J, Blumberg WE (1979) The orientational freedom of molecular probes. The orientation factor in intramolecular energy transfer. *Biophys J* 26:161-193
Erratum in: *Biophys J* 30:365, ISSN 0006-3495
- de Almeida RF, Loura LMS, Prieto M (2009) Membrane lipid domains and rafts: current applications of fluorescence lifetime spectroscopy and imaging. *Chem Phys Lipids* 157:61-77, ISSN 0009-3084
- Filipe HAL, Moreno MJ, Loura LMS (2011). Interaction of 7-nitrobenz-2-oxa-1,3-diazol-4-yl-labeled fatty amines with 1-palmitoyl, 2-oleoyl-*sn*-glycero-3-phosphocholine bilayers: a molecular dynamics study. *J Phys Chem B* 115: 10109-10119, ISSN 1520-6106
- Franks NP (1976) Structural analysis of hydrated egg lecithin and cholesterol bilayers. I. X-ray diffraction. *J Mol Biol* 100:345-358, ISSN 0022-2836
- Franová M, Repáková J, Čapková P, Holopainen JM, Vattulainen I (2010) Effects of DPH on DPPC-cholesterol membranes with varying concentrations of cholesterol: from local perturbations to limitations in fluorescence anisotropy experiments. *J Phys Chem B* 114:2704-2711, ISSN 1520-6106
- Gennis RB (1989) Biomembranes: molecular structure and function. Springer, New York, ISBN 0387967605
- Gimpl G, Gehrig-Burger K (2011) Probes for studying cholesterol binding and cell biology. *Steroids* 76:216-231, ISSN 0039-128X
- Gullapalli RR, Demirel MC, Butler PJ (2008) Molecular dynamics simulations of DiI-C₁₈(3) in a DPPC lipid bilayer. *Phys Chem Chem Phys* 10:3548-3560, ISSN 1463-9076
- Harriman A, Izzet G, Ziessel R (2006) Rapid energy transfer in cascade-type bodipy dyes. *J Am Chem Soc* 128:10868-10875, ISSN 0002-7863
- Herrenbauer M (2002) Biosorption of Polycyclic Aromatic Hydrocarbons (PAH) to microorganisms and liposomes. Shaker, Aachen, ISBN 3826599039
- Hinner MJ, Marrink SJ, de Vries AH (2009) Location, tilt, and binding: a molecular dynamics study of voltage-sensitive dyes in biomembranes. *J Phys Chem B* 113:15807-15819, ISSN 1520-6106
- Hoff B, Strandberg E, Ulrich AS, Tieleman DP, Posten C (2005) ²H-NMR study and molecular dynamics simulation of the location, alignment, and mobility of pyrene in POPC bilayers. *Biophys J* 88:1818-1827, ISSN 0006-3495

- Hölttä-Vuori M, Uronen RL, Repáková J, Salonen E, Vattulainen I, Panula P, Li Z, Bittman R, Ikonen E (2008) BODIPY-cholesterol: a new tool to visualize sterol trafficking in living cells and organisms. *Traffic* 9:1839–1849, ISSN 1398-9219
- Huster D, Müller P, Arnold K, Herrmann A (2001) Dynamics of membrane penetration of the fluorescent 7-nitrobenz-2-oxa-1, 3-diazol-4-yl (NBD) group attached to an acyl chain of phosphatidylcholine. *Biophys J* 80:822–831, ISSN 0006-3495
- Kachel K, Asuncion-Punzalan E, London E (1998) The location of fluorescence probes with charged groups in model membranes. *Biochim Biophys Acta* 1374:63–76, ISSN 0006-3002
- Kaiser RD, London E (1998) Location of diphenylhexatriene (DPH) and its derivatives within membranes: comparison of different fluorescence quenching analyses of membrane depth. *Biochemistry* 37:8180–8190, ISSN 0006-2960
- Kyrychenko A (2010a) A molecular dynamics model of rhodamine-labeled phospholipid incorporated into a lipid bilayer. *Chem Phys Lett* 485:95–99, ISSN 0009-2614
- Kyrychenko A, Wu F, Thummel RP, Waluk J, Ladokhin AS (2010b) Partitioning and localization of environment-sensitive 2-(2'-pyridyl)- and 2-(2'-pyrimidyl)-indoles in lipid membranes: a joint refinement using fluorescence measurements and molecular dynamics simulations. *J Phys Chem B* 114:13574–13584, ISSN 1520-6106
- Kyrychenko A, Sevriukov IY, Syzova ZA, Ladokhin AS, Doroshenko AO (2011) Partitioning of 2,6-Bis(1H-Benzimidazol-2-yl)pyridine fluorophore into a phospholipid bilayer: Complementary use of fluorescence quenching studies and molecular dynamics simulations. *Biophys Chem* 154:8–17, ISSN 0301-4622
- Lakowicz, JR (2006) Principles of Fluorescence Spectroscopy, 3rd Ed. Springer, ISBN 978-0-387-31278-1, New York
- Lentz BR (1989) Membrane “fluidity” as detected by diphenylhexatriene probes. *Chem Phys Lipids* 50:171–190, ISSN 0009-3084
- Lentz BR (1993) Use of fluorescence probes to monitor molecular order and motions within liposome bilayers. *Chem Phys Lipids* 64:99–116, ISSN 0009-3084
- López Cascales JJ, Huertas ML, García de la Torre J (1997) Molecular dynamics simulation of a dye molecule in the interior of a bilayer: 1, 6-diphenyl-1, 3, 5-hexatriene in dipalmitoylphosphatidylcholine. *Biophys Chem* 69:1–8, ISSN 0301-4622
- Loura LMS, Prates Ramalho JP (2007) Location and dynamics of acyl chain NBD-labeled phosphatidylcholine (NBD-PC) in DPPC bilayers. A molecular dynamics and time-resolved fluorescence anisotropy study. *Biochim Biophys Acta* 1768:467–478, ISSN 0006-3002
- Loura LMS, Fedorov A, Prieto M (2001) Exclusion of a cholesterol analog from the cholesterol-rich phase in model membranes. *Biochim Biophys Acta* 1511:236–243, ISSN 0006-3002
- Loura LMS, Fernandes F, Fernandes AC, Prates Ramalho JP (2008) Effects of fluorescent probe NBD-PC on the structure, dynamics and phase transition of DPPC. A molecular dynamics and differential scanning calorimetry study. *Biochim Biophys Acta* 1778:491–501, ISSN 0006-3002
- Loura LMS, Palace Carvalho AJ, Prates Ramalho JP (2010a) Direct calculation of Förster orientation factor of membrane probes by molecular simulation. *J Mol Struct (THEOCHEM)* 946:107–112, ISSN 0166-1280

- Loura LMS, Prieto M, Fernandes F (2010b) Quantification of protein-lipid selectivity using FRET. *Eur Biophys J* 39:565-578, ISSN 0175-7571
- Loura LMS, Fernandes F, Prieto M (2010c) Membrane microheterogeneity: Förster resonance energy transfer characterization of lateral membrane domains. *Eur Biophys J* 39:589-607, ISSN 0175-7571
- Maier O, Oberle V, Hoekstra D (2002) Fluorescent lipid probes: some properties and applications (a review). *Chem Phys Lipids* 116:3-18, ISSN 0009-3084
- Marrink SJ, Risselada HJ, Yefimov S, Tieleman DP, de Vries AH (2007) The MARTINI forcefield: coarse grained model for biomolecular simulations. *J Phys Chem B* 111:7812, ISSN 1520-6106
- Mitchell DC, Litman BJ (1998) Molecular order and dynamics in bilayers consisting of highly polyunsaturated phospholipids. *Biophys J* 74:879-891, ISSN 0006-3495
- Mukherjee S, Raghuraman H, Dasgupta S, Chattopadhyay A (2004) Organization and dynamics of *N*-(7-nitrobenz-2-oxa-1, 3-diazol-4-yl)-labeled lipids: a fluorescence approach. *Chem Phys Lipids* 127:91-101, ISSN 0009-3084
- Repáková J, Čapková P, Holopainen JM, Vattulainen I (2004) Distribution, orientation, and dynamics of DPH probes in DPPC bilayer. *J Phys Chem B* 108:13438-13448, ISSN 1520-6106
- Repáková J, Holopainen JM, Morrow MR, McDonald MC, Čapková P, Vattulainen I (2005) Influence of DPH on the structure and dynamics of a DPPC bilayer. *Biophys J* 88:3398-3410, ISSN 0006-3495
- Repáková J, Holopainen JM, Karttunen M, Vattulainen I (2006) Influence of pyrene-labeling on fluid lipid membranes. *J Phys Chem B* 110:15403-15410, ISSN 1520-6106
- Royer CA, Scarlata SF (2008) Fluorescence approaches to quantifying biomolecular interactions. *Methods Enzymol* 450:79-106, ISSN 0076-6879
- Scheidt HA, Müller P, Herrmann A, Huster D (2003) The potential of fluorescent and spin-labeled steroid analogs to mimic natural cholesterol. *J Biol Chem* 278:45563-45569, ISSN 0021-9258
- Shaw JE, Epand RF, Epand RM, Li Z, Bittman R, Yip CM (2006) Correlated fluorescence-atomic force microscopy of membrane domains: structure of fluorescence probes determines lipid localization. *Biophys J* 90:2170-2178, ISSN 0006-3495
- Simons K, Ikonen E (1997) Functional rafts in cell membranes. *Nature* 387:569-572, ISSN 0028-0836
- Skaug MJ, Longo ML, Faller R (2009) Computational studies of Texas Red-1,2-dihexadecanoyl-*sn*-glycero-3-phosphoethanolamine - model building and applications. *J Phys Chem B* 113:8758-8766, ISSN 1520-6106
- Skaug MJ, Longo ML, Faller R (2011) The impact of Texas Red on lipid bilayer properties. *J Phys Chem B* 115:8500-8505, ISSN 1520-6106
- Somerharju P (2002) Pyrene-labeled lipids as tools in membrane biophysics and cell biology. *Chem Phys Lipids* 116:57-74, ISSN 0009-3084
- Song NC, Livanec PW, Klauda JB, Kuczera K, Dunn RC, Im W (2011) Orientation of fluorescent lipid analogue BODIPY-PC to probe lipid membrane properties: insights from molecular dynamics simulations. *J Phys Chem B* 115:6157-6165, ISSN 1520-6106
- Straume M, Litman BJ (1987) Equilibrium and dynamic structure of large, unilamellar, unsaturated acyl chain phosphatidylcholine vesicles. Higher order analysis of 1, 6-

- diphenyl-1, 3, 5-hexatriene and 1-[4-(trimethylammonio)phenyl]- 6-phenyl-1, 3, 5-hexatriene anisotropy decay. *Biochemistry* 26:5113-5120 Erratum in: *Biochemistry* 26:8030, ISSN 0006-2960
- Stryer L (1978) Fluorescence energy transfer as a spectroscopic ruler. *Annu Rev Biochem* 47:829-846, ISSN 0066-4154
- van der Meer BW, Coker G, Simon Chen S (1994) Resonance energy transfer, theory and data. VCH Publishers, ISBN-10: 0471185892, New York
- Wolf DE (1988) Probing the lateral organization and dynamics of membranes. In: Loew LM (ed) *Spectroscopic membrane probes*, vol I. CRC, Boca Raton, pp 193-220, ISBN 0849345359
- Worcester DL, Franks NP (1976) Structural analysis of hydrated egg lecithin and cholesterol bilayers. II. Neutrol diffraction. *J Mol Biol* 100:359-378, ISSN 0022-2836
- Zhang Y, Li X, Becker KA, Gulbins E (2009) Ceramide-enriched membrane domains - structure and function. *Biochim Biophys Acta* 1788:178-183, ISSN 0006-3002

IntechOpen



Biophysics

Edited by Dr. Prof. Dr. A.N. Misra

ISBN 978-953-51-0376-9

Hard cover, 220 pages

Publisher InTech

Published online 21, March, 2012

Published in print edition March, 2012

Biophysics is a vast cross-disciplinary subject encompassing the fields of biology, physics and computational biology etc in microbes, plants, animals and human being. Wide array of subjects from molecular, physiological and structural are covered in this book. Most of these chapters are oriented toward new techniques or the application of techniques in the novel fields. The contributions from scientists and experts from different continents and countries focuss on major aspects of biophysics. The book covers a wide range of topics reflecting the complexity of the biological systems. Although the field of biophysics is ever emerging and innovative, the recent topics covered in this book are contemporary and application-oriented in the field of biology, agriculture, and medicine. This book contains mainly reviews of photobiology, molecular motors, medical biophysics such as micotools and hoemodynamic theory.

How to reference

In order to correctly reference this scholarly work, feel free to copy and paste the following:

Luís M.S. Loura, A.J. Palace Carvalho and J.P. Prates Ramalho (2012). Recent Developments in the Study of the Behavior of Fluorescent Membrane Probes in Lipid Bilayers: Molecular Dynamics Approach, Biophysics, Dr. Prof. Dr. A.N. Misra (Ed.), ISBN: 978-953-51-0376-9, InTech, Available from:
<http://www.intechopen.com/books/biophysics/recent-developments-in-the-study-of-the-behavior-of-fluorescent-membrane-probes-in-lipid-bilayers-mo>

INTECH
open science | open minds

InTech Europe

University Campus STeP Ri
Slavka Krautzeka 83/A
51000 Rijeka, Croatia
Phone: +385 (51) 770 447
Fax: +385 (51) 686 166
www.intechopen.com

InTech China

Unit 405, Office Block, Hotel Equatorial Shanghai
No.65, Yan An Road (West), Shanghai, 200040, China
中国上海市延安西路65号上海国际贵都大饭店办公楼405单元
Phone: +86-21-62489820
Fax: +86-21-62489821

© 2012 The Author(s). Licensee IntechOpen. This is an open access article distributed under the terms of the [Creative Commons Attribution 3.0 License](https://creativecommons.org/licenses/by/3.0/), which permits unrestricted use, distribution, and reproduction in any medium, provided the original work is properly cited.

IntechOpen

IntechOpen